

# Autopsy on an RF-Processed X-band Travelling Wave Structure

F. Le Pimpec, S. Harvey, R.E. Kirby, F. Marcelja  
 SLAC, 2575 Sand Hill Road, Menlo Park CA 94025 , USA

## Abstract

In an effort to locate the cause(s) of high electric-field breakdown in x-band accelerating structures, we have cleanly-autopsied (no debris added by post-operation structure disassembly) an RF-processed structure. Macroscopic localization provided operationally by RF reflected wave analysis and acoustic sensor pickup was used to connect breakdowns to autopsied crater damage areas. Surprisingly, the microscopic analyses showed breakdown craters in areas of low electric field. High currents induced by the magnetic field on sharp corners of the input coupler appears responsible for the extreme breakdown damage observed.

## 1 INTRODUCTION

The Next Linear Collider (NLC) accelerating structures, running at 11.424 GHz, are expected to hold a steady operational surface gradient of 73 MV/m, without breakdown arcing. A development program for the required structure has been in progress at SLAC for several years. Possible RF structure candidates, Travelling Wave (TW) and Standing Wave (SW) are tested in a specially dedicated linac at SLAC, the Next Linear Collider Test Accelerator (NLCTA). So far, mixed results have been obtained during high electric field-processing of structures, cf Fig. 1. Part of the success in reaching the required gradient has been the great improvement in cleaning and handling the structure prior to RF processing. Results of the breakdown pattern analysis via RF or acoustic sensors Fig.2, have led to the necessity to cut open the structure. In this paper we will present some of the results of the analysis of the autopsy of the 53 cm long T53Vg3R TW structure.

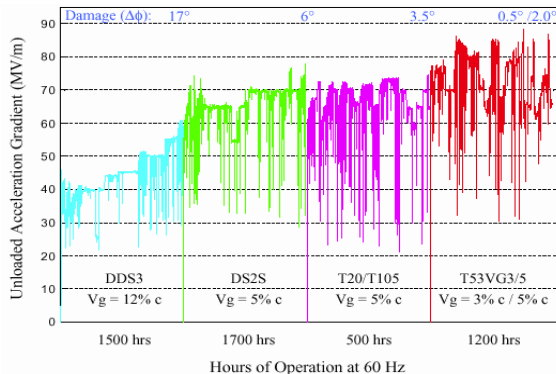


Figure 1: History operation at NLCTA of some 11.424 GHz TW structures

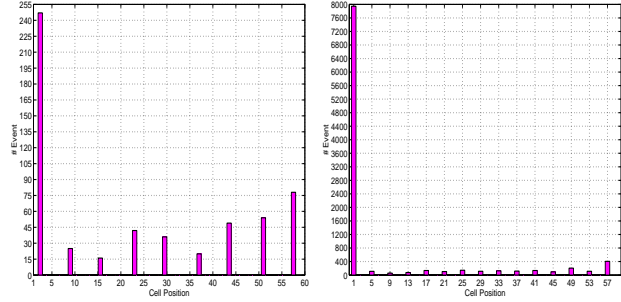


Figure 2: Example of damage localization in T53Vg3R (left) - T53Vg3RA (right) during operation

## 2 RESULTS OF THE ANALYSIS AND DISCUSSION

During RF breakdown few kA/A of electrons/ions are emitted inside a cell. The kinetic energy of electrons can be up to 100 keV and ions up to few keV [1] [2]. Among the interactions of those particles with the surface, few of them might directly cause damage to the surface such as surface heating and sputtering.

The breakdown pattern localization Fig.2 reveals that most of the breakdown are occurring in the input coupler (IC) of the TW. In Fig.3 we can see that the input coupler is divided into two parts the waveguide section, left side of the picture and the cell side in the center. The feature separating the waveguide side and the cell side is denominated "horns". The gap between the top and bottom horn is  $\sim 9$ mm.

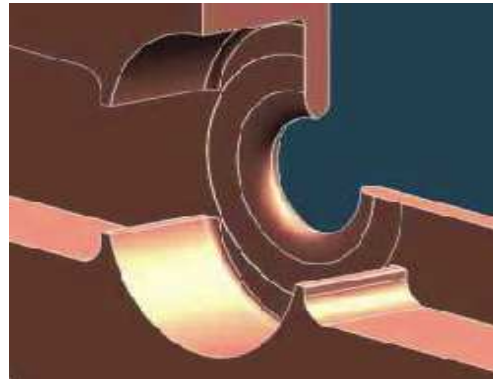


Figure 3: Input coupler design. The center is the cavity side with the first iris

Fig.4, 5 and 6 reveal a very interesting pattern of damage. The craters on the floor of the IC, Fig.4, are mainly located along the imaginary circles connecting the two faces of the horns. Closing up to the horns and focusing on the

details, one can observe droplets of copper [3]. Craters appears on all the sides of the horns, with a density higher in the face side than the waveguide or cavity side. Looking more closely of the edges of the four horns has revealed that the edge on the waveguide side, Fig.5, shows little damage. In the contrary the edge on the cell side shows a chaos of features, Fig. 6, with sharp and melted objects. The dimension bar in the right picture of Fig.6 is  $\sim 10\mu m$ .

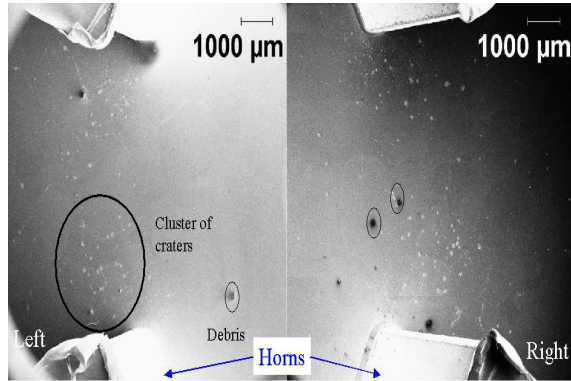


Figure 4: Pitting due to RF breakdown on the floor of the Input coupler. The iris is in between the horns.

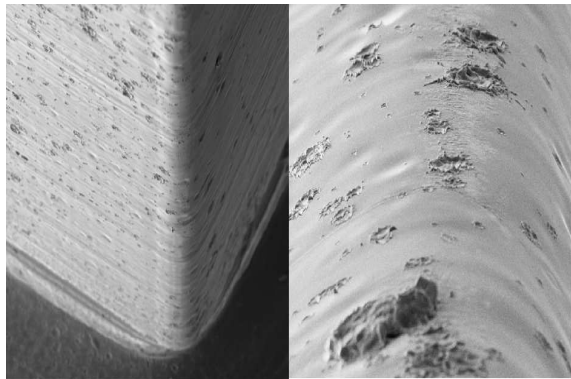


Figure 5: Typical damage on the waveguide side of a horn of the IC

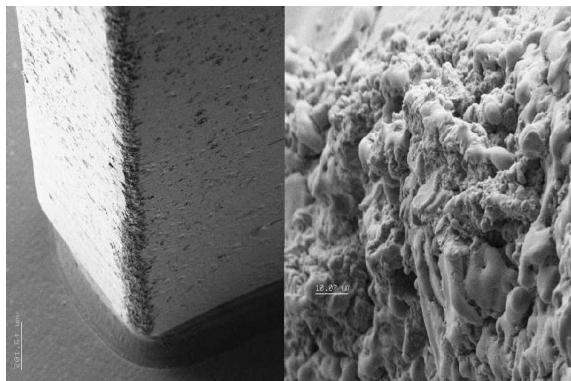


Figure 6: Typical damage on the Cell side of a horn of the IC

The observation of the damages on the horns is coherent with the acoustic sensors analysis. Also pictures taken during breakdown show clearly after averaging over 100 of breakdowns 4 spots in the approximative location of the horns [4]. At first Ion bombardement and sputtering might

be invoked to explain the damages. However, the horns lies in a very low electric field area, and the vacuum is of the order of  $3.10^{-9}$  Torr. It is then not possible to explain how such a low gas density and kinetic energy might start a breakdown leading to the so seen damages. It is also not possible to explain the very localization on the edge of the cavity side of the horns Fig.6. During processing, the RF pulse went from 50 ns to 400 ns carrying up to 100 MW of power. Part of this energy is dumped in the Cu in form of heat or directly or by the induced current due to the high magnetic field 0.7 MA/m at 400 ns pulse length [5]. Along the edge ( $76\mu m$  radius) this RF pulse heating leads to an increase of temperature up to  $130\text{ }^\circ\text{C}$ . It is clear that this temperature do not cause the observed damage. However, it might induce thermal fatigue in the Cu, inducing formations of cracks, as observed in [6], and leading in roughening of the edge. As the surface becomes rougher, the local resistivity of the Cu increases leading to a higher temperature maybe up to the melting point ( $1083\text{ }^\circ\text{C}$ ). At this temperature, the vapor pressure of the Cu is  $\sim 3.10^{-4}$  Torr [7]. This gas can now be ionized by the electrons coming form the surface and back bombard the horns. As a result, raising up the temperature and sputtering the surface. We might, in addition, explain the droplet of Cu seen at the surface of the floor. The patterns of craters on the floor, Fig.4, seems to follow the high magnetic field line. As we move toward the center the density of craters diminish and increase again as the electric field start to be consequent Fig 7.

SEM (secondary electron microscopy) Fig. 7 shows the damage on the upstream side and the downstream side of the iris, respectif to the displacement of the NLCTA electron beam. On both sides etch pits can be seen as well as craters. However, the density of craters is much higher in the upstream side. Many craters are also located in the grain boundary. A particle search in and out of the craters shows MnS located in and out of them. Most of this inclusions are located in the grain boundary. The analysis of the contents of the craters shows mainly pure Cu. The black spots on the upstream side is carbon. An Auger analysis of the surface, not including those spots, shows heavy contamination by carbon of this iris [3]. Carbon contamination due to electron bombardement is a well known problem, [8]. There is no such contamination in iris 28 further down the structure [3].

As we move toward the output coupler (OC), the activity on the irises decreases, endoscope (boroscope) monitoring. Fig.8 shows the sparse activity on the 28th iris of the structure. As we looked for particles/inclusions on the surface and at the grain boundary, we did not find MnS. However, some other sulfur compound were found [3], as the atypical one shown in Fig.8.

The cells used to make the structure are bonded and then brazed in a stainless steel (SS)  $\text{H}_2$  furnace at  $\sim 1020\text{ }^\circ\text{C}$ . The Sulfur (S) composition is 0.03 weight % in stainless steel. Other material like Mn, Cr, Ni are also used in the making of SS. The solubility of sulfur in copper is

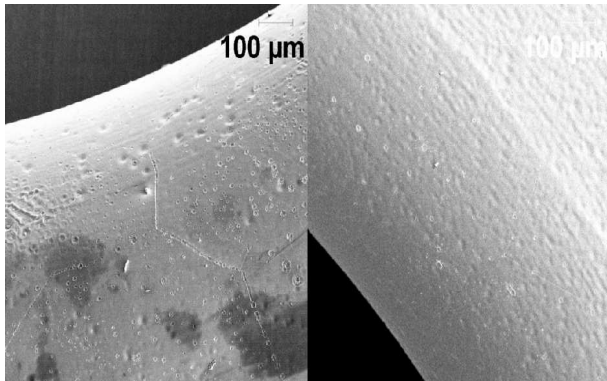


Figure 7: Activity on the 1<sup>st</sup> iris, Upstream side left picture and downstream side right picture

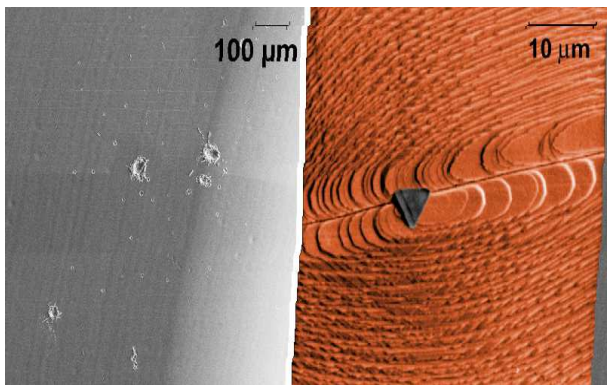


Figure 8: Activity on the 28<sup>th</sup> iris, Upstream side. CrS inclusion at a twin boundary, right picture

very high at this temperature and significant at a few hundred °C. Hence, a significant amount of S can get into the copper. After its fabrication, the structure is vacuum baked in a SS pot at 650°C for few days, in order to desorb the H<sub>2</sub>. Metals might be present in the atmosphere of the H<sub>2</sub> furnaces and bakeout pot at this given temperature, with vapor pressures of 10<sup>-5</sup> Torr for Mn, 10<sup>-11</sup> Torr for Cr, 10<sup>-1</sup> Torr for Ca and below 10<sup>-11</sup> Torr for Ni [7]. At 300°C and above the S concentrates at the grain boundaries of the Cu. The S also start migrating to the surface at low temperature 75°C [9]. The Model for sulfur compound formation is that the sulfur getters the metal vapor out of the furnace atmosphere to form crystals/inclusions at/near the grain boundaries. A particle search on the IC reveals that ~80% of the particles are Mn-S. On the very next iris the proportion falls to ~50%. The search in the 28<sup>th</sup> cell shows no Mn-S but S-compounds are present at ~50%. Finally the search on the last cell in front of the OC shows Mn-S and other S-compounds. Finally in all the cases, other particles are compounds based on C, Al and Si not excluding the presence of Mn or S or other elements. This model might explain the sulfur compound formation, but the understanding of the distribution along the structure of those elements is under investigation.

### 3 CONCLUSION

Following our autopsy many studies and simulation led to the decision of rounding the edge to 3mm instead of 76 μm radius in order to avoid the thermal fatigue roughening mechanism. It is believed that the new design of the IC and OC implementing this rounding will cure our breakdown problem in those couplers. Also, machining a 3mm edge radius should leave the surface extremely smooth. We have shown on an identical input coupler of T53Vg3R, Fig.9, that the 4 edges of the cavity side of the horns present a roughness after machining. Following the etching and thermal processing, that sees the structure, do not removed this roughness. In a contrary, the edge on the waveguide side of the horns are well finished.

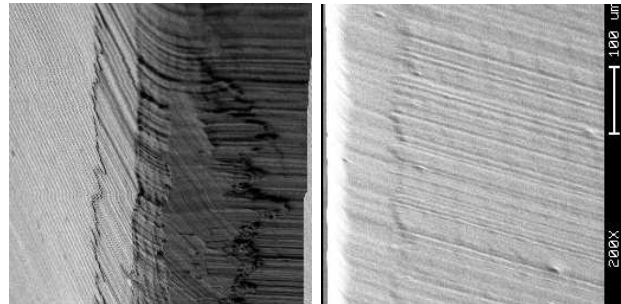


Figure 9: Surface of the edge, cell side, of a horn after machining (left) and after 60'' etch and thermal processing

In order to confirm the sharp corner problem two other structures will be cut open. The T53Vg3RA has also reached the desired 73 MV/m but the IC were responsible of more than 75% of the breakdown Fig.2. It is then important to compare the two structures. Finally the wake-field damping slots in a cell, of an NLC type RF-structure, DDS3 cf Fig.1, will be cut open and analyse. Those damping slots might have sharp and not de-burred corners leading to the understanding of DDS3 poor performance.

### 4 REFERENCES

- [1] V. Dolgashev, S. Tantawi. Simulations of currents in X-band accelerator structures using 2D and 3D particle-in-cell code. In *PAC 2001*, 2001.
- [2] V. Dolgashev private communication.
- [3] F. Le Pimpec, S. Harvey, R. Kirby, F. Marcelja . Results from the surface analysis of the autopsy of the T53VG3R structure. In *ISG8*, 2002.
- [4] M. Ross et al. Measurement of RF Breakdown in X-band Structures. In *LC02 Workshop SLAC*, 2002.
- [5] V. Dolgashev et al. SW Processing, Pulse Heating. In *ISG8*, 2002.
- [6] D. Pritzkau. *thesis : RF Pulsed Heating*. SLAC-report-577.
- [7] A. Berman. *Vacuum Engineering Calculations, Formulas, and Solved Exercises*. Academic Press, 1992.
- [8] K.I. Sciffmann. *Nanotechnology*, 4:163, 1993.
- [9] B. Singh et al. AES study of sulfur surface segregation on polycrystalline copper. *JVST*, 17(1):29–33, 1980.